MAIN AND NORMAL CUTTING FORCES BY MACHINING WOOD OF *PINUS SYLVESTRIS*

Bolesław Porankiewicz,[a,*] Bengt Axelsson,[b] Anders Grönlund,[c] and Birger Marklund [c]

In this work the multi-factor, non-linear dependencies between main (tangential) F_C (N) and normal (radial) F_N (N) cutting forces and eight machining parameters by sawing simulation of wood of *Pinus sylvestris* L. were evaluated. The relationships are graphically illustrated and discussed. Evidence of several contradictions was found relative to results from available literature.

Keywords: Multi-factor non-linear statistical dependencies; Main cutting force; Normal cutting force; Circular sawing; Wood; Scotch pine

Contact information: a: University of Zielona Góra; b: Westinghouse Electric Company European LWR Fuel Business, SE-721 63 Västerås, Sweden; c: Luleå University of Technology;
**Corresponding author: poranek@amu.edu.pl*

INTRODUCTION

Although *Pinus sylvestris* L. is the most frequently analyzed wood species with respect to cutting forces in sawing experiments, the problem of prediction of reliable values of tangential F_C and radial F_N cutting forces for specific sawing conditions, according to the method employing a specific cutting resistance K ($N \cdot mm^{-2}$) and correction coefficients C_R, C_δ, C_ρ, C_{AP}, C_{VC}, C_{MC}, C_T, as expressed by Equations (1) and (2) is far from being solved (Afanasev 1961; Amalitskij and Lûbčenko 1977; Beršadskij 1967; Deševoj 1939; Orlicz 1982).

$$F_c = a_p \cdot w_c \cdot K \cdot C_r \cdot C_\delta \cdot C_\rho \cdot C_{ap} \cdot C_{vc} \cdot C_{mc} \cdot C_T \quad \text{(N)} \qquad (1)$$

In equation (1) the terms are defined as follows:

a_P - Thickness of the cutting layer (also known as uncut chip thickness, mm,
w_C - Width of cutting (mm),
$K=f(\varphi_V)$ - Specific cutting resistance ($N \cdot mm^{-2}$, MPa),
C_R - Coefficient of wood species, for *Pinus sylvestris* L. wood $C_R=1$,
$C_\delta=f(\delta_F)$ - Coefficient of cutting angle δ_F,
$C_\rho=f(\rho$ or $VB)$ - Coefficient of the cutting edge dullness (ρ, VB),
ρ - Radius of the cutting edge round up (μm),
VB - Recession of the cutting edge (μm),
$C_{AP}=f(a_P)$ - Coefficient of a thickness of a cutting layer (chip thickness) a_P,
$C_{VC}=f(v_C)$ - Coefficient of a cutting velocity v_C,
$C_{MC}=f(m_C)$ - Coefficient of a moisture content of wood m_C,
$C_T=f(T)$ - Coefficient of a wood temperature T.

$$F_N = C_{FN} \cdot F_C \quad \text{(N)} \qquad (2)$$

In Eq. (2) the new term C_{FN} , which is a function of ρ or VB, is the coefficient of the normal force F_N.

In authors' opinion, the reason that the problem has not yet been adequately solved is due to the large number of cutting parameters and their interactions involved, and also due to the fact that Equation (1) does not take into account mechanical properties, as well as wood density, instead of an arbitrarily assumed value of the wood species correction coefficient C_R. The wood of the *Pinus sylvestris* L., may differ considerably in physical and mechanical properties, resulting in a large dispersion of predicted cutting forces in comparison to observed ones, reported as high as 40 % and more (Orlicz 1982). The specific cutting resistance K, evaluated as an average value, cannot take into account differences in cutting resistance generated by such factors as: - early and late wood of growth rings; - sap- and heart-wood; - reaction wood; - fresh knots; - and wood near to fresh knots. The exact cutting conditions of experiments, which had been used for evaluation of the base specific cutting resistances K and correction coefficients (C_δ, C_ρ, C_{AP}, C_{VC}, C_{MC}, C_T), as reported in the literature (Afanasev 1961; Amalitskij and Lûbčenko 1977; Beršadskij 1967; Deševoy 1939; Orlicz 1982), remain unknown (or not available), and more, it seems that they were not supported by any multi-factor experiment. It also cannot be excluded that many interactions exist among the dependencies of the main F_C and normal F_N cutting forces upon machining parameters, and these were not taken into account in previous works. Therefore the method of evaluation of cutting forces, based on equation (1), appears to have involved rather rough approximations of the wood cutting theory. Incomplete sets of independent variables have been considered in the published works, and there has been inadequate attention paid to having the same range of their variation in evaluation of formulas of dependencies between the main cutting force F_C as well as normal cutting force F_N, making machining parameters difficult to compare.

It has been known from earlier studies (Amalitskij and Lûbčenko 1977; Kivimaa 1961) that the normal cutting force F_N does not follow the main force F_C; therefore the equation (2), with coefficients' C_{FN} dependency upon the main cutting force F_C and cutting edge recession, is far from the truth.

Instead of exact numbers, a use of qualitative word descriptions of the cutting edge state, such as, for example, "sharp," "moderately dull," and "dull" is not satisfactory for precise analysis. The words "sharp" and "dull," from the point of view of cutting edge round up ρ or the cutting edge recession VB, does not have the same meaning for rough (primary brake-down) and precise (super thin) circular sawing.

A tabular form of values of the specific cutting resistance K and the correction coefficients (C_δ, C_ρ, C_{AP}, C_{VC}, C_{MC}, C_T), defining Equation (1) for *Pinus sylvestris* L. wood, in most published works, sufficient for very rough estimation, needs interpolation when a number lying between values given in a table is needed. This disadvantage of the method, generating an error for variables that are undefined by mathematical function, non-linear relationships, was improved in the program Wood_Cutting (Porankiewicz 2011) for cutting forces calculation, in which statistical formulas for all basic values of

the specific cutting resistances and the correction coefficients, determining formula (1) were evaluated.

The multi-variable statistical relationship, namely Equations (3) though (5), between the main cutting force F_C and eight cutting parameters $F_C=f(\rho, \gamma_F, \varphi_V, a_p, v_C, D, m_C, T)$ was presented in the work Axelsson et al. (1993),

$$F_C=-7.37+A_1+15.61\cdot\varphi_V-2.6\cdot\varphi_V^3+1.31\cdot\rho+0.2\cdot v_C+A_2 \quad \text{(N)} \quad (3)$$

where new terms in Equation (3) are:

$$A_1=a_P\cdot(0.38\cdot D-224.5\cdot\gamma_F) \quad (4)$$

$$A_2=m_C\cdot(0.3\cdot\varphi_V-0.01\cdot T) \quad (5)$$

and:

γ_F = Rake angle (rad),
ρ = Cutting edge dullness, represented by cutting edge round up (μm),
φ_V = Angle between the cutting velocity vector v_C and wood grains (Fig. 2, Fig. 5) (0 .. 2.879793) (rad),
a_P = Thickness of cutting layer, known also as the uncut chip thickness (mm),
D = Average wood density (kg·m^{-3}),
m_C = Moisture content (%),
T = Temperature of wood (ºC).

Equations (3) though (5) seem to be the most sophisticated available in the newer literature, having the following interactions: $a_P \cdot \gamma_F$; $a_P \cdot D$; $m_C \cdot \varphi_V$; $m_C \cdot T$. This equation was evaluated from data obtained from an multi-variable circular sawing simulated experiment.

The issue of interpretation of the impact of the cutting velocity v_C on the main F_C and normal F_N cutting forces is controversial in the literature. According to Kivimaa (1950), by free cutting, the influence of the cutting velocity v_C can be neglected. The presumably small linear influence of the factor v_C on the main F_C and normal F_N cutting forces, also for free cutting, due to chip acceleration, was omited in the work McKenzie (1961). However, in the opinion of the authors, slow, free cutting ought not to be directly compared to closed cutting (sawing) by high cutting velocity v_C. A linear component, representing about a 14 % increase of the main cutting force F_C with growth of the cutting velocity v_C, from 15 m·s^{-1} to 40 m·s^{-1}, was reported in the work of Axelsson et al. (1993), based on Equations (3) though (5), indicating that according to theoretical simulation performed the influence of the chip acceleration on the main cutting force F_C can be omitted. The parabolic relationship, presented in the literature (Amalitskij and Lûbčenko 1977; Orlicz 1982), shows a 9 % decrease of the main cutting force F_C with increase of the cutting velocity v_C to 50 m·s^{-1}, and, further a 36 % increase of the main cutting force F_C with growth of the v_C in the range 50 m·s^{-1} to 100 m·s^{-1}. However no explanation of this phenomenon was given. Because circular sawing is very different

from the free cutting, in authors' opinion, the impact of the cutting velocity v_C on the cutting forces F_C and F_N seem also to be different.

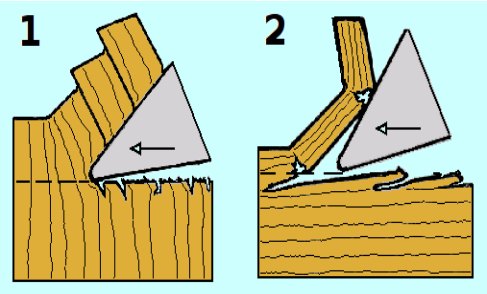

Fig. 1. Chip and fractures formation during cutting: 1 = Perpendicular (φ_K=90°, φ_V=90°, φ_S=90°); 2 = Parallel (φ_K=90°, φ_V=0°, φ_S=0°) to wood grains

The issue of fracture formation and propagation in the contact region of the cutting edge and wood, below and above the cutting plane (Fig. 1) was not considered and not discussed in several published papers related to circular sawing (Afanasev 1961; Amalitskij and Lûbčenko 1977; Beršadskij 1967; Orlicz 1982), by assumption of symmetry of cutting forces changes for wood grain orientation angles φ_V in the ranges of 0° through 90°, and 90° through 180°. A lack of such symmetry, especially for a tool that is not sharp, has been reported (Axelsson et al. 1993; Porankiewicz et al. 2007). In the authors' opinion, an explanation for that phenomenon lies in the issue of fracture formation and propagation. In the case of wood cutting with φ_V lying in the range of 90° through 180° (according to Fig. 2), known as cutting along grains, a fracture tends to propagate above the cutting plane, which is essential also for the formation of the theoretical surface after cutting. In the case of wood grain orientation angle φ_V laying in the range of 0° through 90°, known as cutting against grains, the fractures can propagate below the cutting plane (Fig. 1), resulting in surface damage.

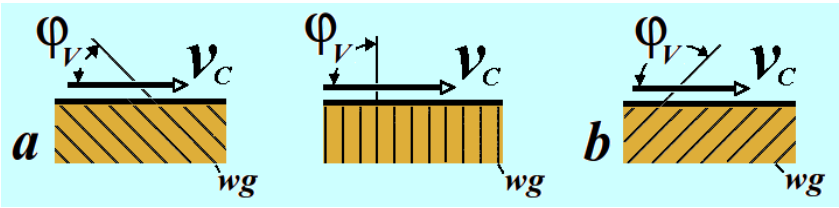

Fig. 2. Wood cutting: a = against grains; b = along grains; wg = with wood grains

Although the main cutting force F_C falls at the moment of creation of a new fracture, an increase of the cutting velocity v_C, can probably limit a fracture formation and propagation in the front of the cutting edge. As a result, an increase of the main force F_C can be observed, especially when the cutting velocity v_C becomes equal or larger than the velocity of propagation of a fracture, which recently has been measured to be about 66 $m \cdot s^{-1}$ (Goli et al. 2007). This might be an explanation for the influence of the cutting velocity v_C on the main cutting force F_C in the range from 50 $m \cdot s^{-1}$ to 100 $m \cdot s^{-1}$, as reported in the literature (Amalitskij and Lûbčenko 1977; Orlicz 1982). The linear

influence of the thickness of the cutting layer a_P (chip thickness), the round up of the cutting edge ρ, the rake angle γ, the moisture content m_C, and the temperature of wood T, presented in the work Axelsson et al. (1993), contradicts information from literature (Amalitskij and Lûbčenko 1977; Orlicz 1982), where all of these influences were reported as being non-linear.

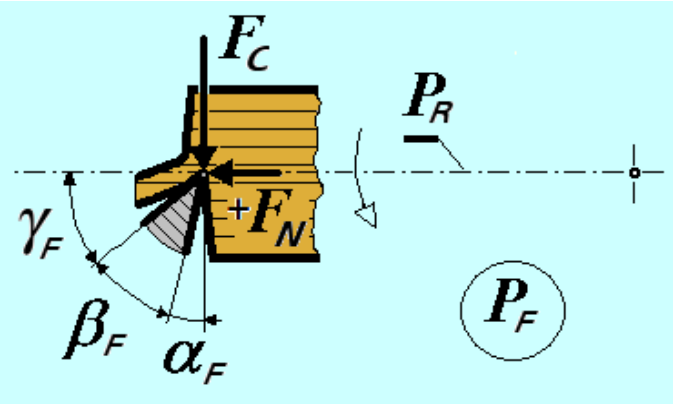

Fig. 3. Main F_C and the normal F_N cutting forces, and stereo-metrical parameters; P_F = Working plain; P_R = Tool reference plain

It has to be mentioned that during sawing, the total main cutting force consists of the main cutting force and load of two side cutting edges. The resistance of the contact of the saw blade, with the surface of the wooden specimen cut, as well as with a sawdust, below the cutting edge, ought rather to be included in the machine spindle load, rather than in the main cutting force F_C, as it has been done through the coefficient of the cutting depth C_H in prevoius publicatoins (Amalitskij and Lûbčenko 1977; Orlicz 1982). Similarly, all forces acting on the work piece and cutting tool outside the cutting region during cutting ought to be considered in the cutting machine theory, rather than in wood cutting process theory.

In the authors' opinion, dynamic characteristics of the set-up for measurement of cutting forces and their calibration, as well the range of variation of independent variables, may also be a reason to explain differentiation of results of the wood cutting forces presented in published works.

The present work attempts to evaluate statistical, non-linear, and multi-variable dependencies of the main $F_C = f(\rho, \gamma_F, \varphi_V, a_p, v_C, D, m_C, T)$, as well as the normal $F_N = f(\rho, \gamma_F, \varphi_V, a_p, v_C, D, m_C, T)$ cutting forces (Fig. 3), during rotational cutting (circular sawing simulating) of the wood of *Pinus sylvestris*.

EXPERIMENTAL

Experiments were performed on the measuring test stand shown in Fig. 4, at Luleå University of Technology, Wood Technology Faculty in Skellefteå, Sweden. The wood specimen 1 was mounted in the holder 4, on the rotating arm 5, powered through the belt transmission 7, from a 4/1400 RPM electrical motor 6, coupled with a stepless variator Eurodrive Type RX81 VU 3 DT 112M-4 COM 82.50555. The piezoelectric

transducers 3, were mounted to the cutting tool holder, which was fixed to the tool support 11, powered through the type Servomoler Berger LAHR VRDM 564/50 LNA0027 4088 1,7Ω 0,95A 12070 015000 servomotor 9, and the feed screw 10. The X and Y cutting force analog signal components from piezoelectric transducers 3 were sent to type 2635, Brüel & Kjaer charge amplifiers, passing through an A/D converter, and stored in PC memory in digital form. The sampling rate was of 25kHz. The sampling process and the feed speed were triggered at the same time from the PC.

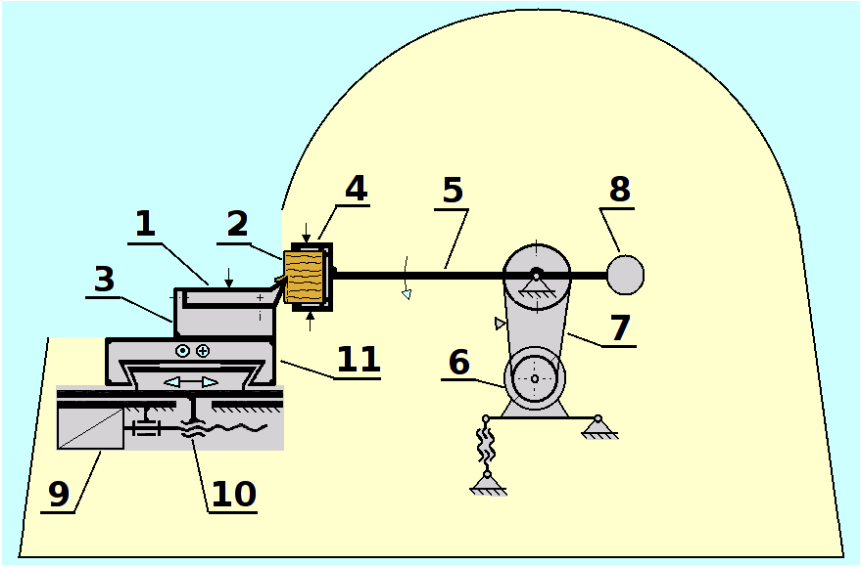

Fig. 4. General scheme of measuring system: 1 – Cutting tool; 2 – Work-piece; 3 – 3D piezoelectric load cells; 4 - Work piece holder; 5 - Rotating arm; 6 - Motor; 7 - Transmission belt; 8 - Balance mass; 9 - Servo-Motor; 10 - Feed screw mechanism; 11 - Tool support

The following machining parameters were applied in the experiment (where the values in parentheses "( )" shows the minimum and maximum values of independent variables, and " .." marks show that more variables in a range were analyzed). Parameters of the experiment were as follows:

1. Mechanical and physical properties of wood specimens:
- Wood density, for m_C=8%, D (372 .. 735) kg·m^{-3},
- Moisture content m_C (8 .. 133) %,
- Temperature of wood T (-15, 20)°C,
- Wood specimen dimensions 70 mm, 70 mm and 170 mm: height, width and length respectively.

2. Machining parameters:
- Cutting edge round up ρ (5, 20) μm,
- Contour wedge angle β_F(0.87633, 1.04545, 1.226268) rad, (50.21, 59.9, 70.26)°, (Fig. 3),
- Contour cutting angle δ_F(1.05086, 1.21999, 1.4008) rad, (60.21, 69.9, 80.26)°,
- Contour rake angle γ_F (0.17, 0.35081, 0.51993) rad, (9.74, 20.1, 29.79)°, (Fig. 3),
- Contour clearance angle α_F (0.174533) rad, (10)°, (Fig. 3),

- Cutting edge inclination angle λ_P=0°,
- Maximum cutting radius r_C=535 mm,
- Spindle rotational speed n (268, 714) min^{-1},
- Average cutting velocity v_C (14.916, 39.741) m·s^{-1},
- Feed speed v_F (0.004 .. 0.382) m·min^{-1},
- Thickness of cutting layer (chip thickness) a_p (0.05, 0.15, 0.5) mm,
- Feed per edge f_Z (0.05, 0.15, 0.5) mm,
- Cutting depth in feed direction g_S=7 mm,
- Width of cutting w_C=4.25 mm,
- Number of cutting edges z=1,
- Angle between cutting edge and wood grains (Fig. 5) φ_K=90°,
- Growth rings orientation angle towards cutting edge (Fig. 5) φ_{RT}=0°,
- Wood grain orientation angle φ_V (Fig. 5), equal the cutting plane φ_S angle (Fig. 5), (0, 15, 45, 75, 90, 105, 135, 165)°.

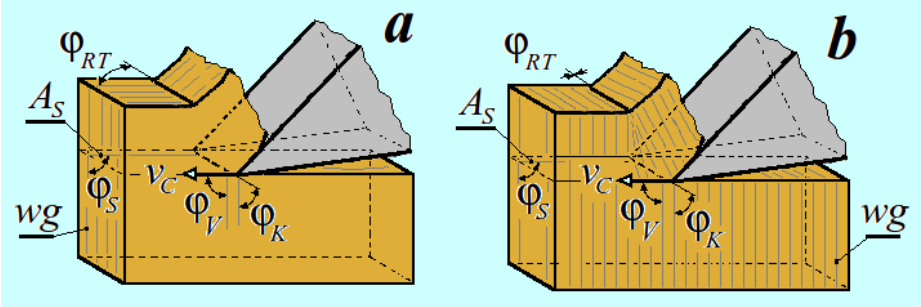

Fig. 5. Orientation angles between wood grains (*wg*) and: φ_V - vector of cutting velocity; φ_K - cutting edge; φ_S - cutting plane; for perpendicular cutting case (φ_K=90°, φ_V=90°, φ_S=90°); by growth rings orientation angle φ_{RT}: a - φ_{RT}=90° (radial); b - φ_{RT}=0° (tangential); A_S - cutting plane

The change of cutting radius generated by the depth of cutting in the range of 0 to 7 mm resulted in negligibly small variation of the cutting speed of 1.4 %.

3. Material of the cutting edge:

The material was a cobalt-chromium-tungsten alloy (Stellite 12). The proper influence of variables was analyzed, especially in the case of incomplete experimental matrix, and the precise data fit, by the highest correlation coefficient R, between predicted and observed values, by the lowest standard deviation S_D, and by the lowest summation of residuals square S_K. Thus one should get an adequate statistical model, of the relations F_C and $F_N=f(\varphi_V, \rho, \gamma_F, a_p, v_C, D, m_C, T)$, by the best fit of the experimental data. In the authors' opinion, additional justification of a choice of a certain type of complicated function makes sense, when several experiments under exactly the same machining conditions have been done in the past. The choice of using a simpler mathematical formula usually results in decreasing approximation quality (lower R, larger S_D and S_K), and also very often results in a reverse impact of less important independent variables.

It must to be pointed out that a statistical equation is valid only for ranges of independent variables chosen within the experimental matrix, especially for incomplete experimental matrices and complicated mathematical formulas with interactions.

In order to evaluate relations F_C and $F_N=f(\varphi_V,\ \rho,\ \gamma_F,\ a_P,\ v_C,\ D,\ m_C,\ T)$, linear formulas and second order multinomial formulas, as well as power and exponential type functions without and with interactions were analyzed in preliminary calculations. The most adequate appeared to be the non-linear, multi-variable Equations (6) though (11),

$$F_C=[a_1+a_2\cdot|\cos(\varphi_V+a_3)|^{a_4}]\cdot P_{A1}+[a_5+a_6\cdot|\sin(\varphi_V+a_7)|^{a_8}]\cdot P_{A2}+a_{27} \quad \text{(N)} \qquad (6)$$

In Eq. (6) the terms P_{A1} and P_{A2} are defined as follows,

$$P_{A1}=a_P^{a_9}\cdot\gamma_F^{a_{10}}\cdot\rho^{a_{11}}\cdot v_C^{a_{12}}\cdot D^{a_{13}}\cdot(a_{14}-e^{mc\cdot a_{15}})^{-1}\cdot(a_{16}-e^{T\cdot a_{17}})^{-1} \qquad (7)$$

$$P_{A2}=a_P^{a_{18}}\cdot\gamma_F^{a_{19}}\cdot\rho^{a_{20}}\cdot v_C^{a_{21}}\cdot D^{a_{22}}\cdot(a_{23}-e^{mc\cdot a_{24}})^{-1}\cdot(a_{25}-e^{T\cdot a_{26}})^{-1} \qquad (8)$$

$$F_N=[b_1+b_2\cdot|\cos(\varphi_V+b_3)|^{b_4}]\cdot P_{B1}+[b_5+b_6\cdot|\sin(\varphi_V+b_7)|^{b_8}]\cdot P_{B2}+b_{27} \quad \text{(N)} \qquad (9)$$

In Eq. (9) the terms P_{B1} and P_{B2} are defined as follows:

$$P_{B1}=b_P^{b_9}\cdot\gamma_F^{b_{10}}\cdot\rho^{b_{11}}\cdot v_C^{b_{12}}\cdot D^{b_{13}}\cdot(b_{14}-e^{mc\cdot b_{15}})^{-1}\cdot(b_{16}-e^{T\cdot b_{17}})^{-1} \qquad (10)$$

$$P_{B2}=b_P^{a_{18}}\cdot\gamma_F^{b_{19}}\cdot\rho^{b_{20}}\cdot v_C^{a_{21}}\cdot D^{b_{22}}\cdot(b_{23}-e^{mc\cdot b_{24}})^{-1}\cdot(b_{25}-e^{T\cdot b_{26}})^{-1} \qquad (11)$$

where φ_V (rad), γ_F (rad), and T (°K) have the respective units.

Estimators for Equations (6) through (11) were evaluated from a complete experimental matrix for variables: ρ, γ_F, a_P, v_C and T and for an incomplete experimental matrix for variables φ_V, m_C and D, containing 412 measuring points (Table 1). During evaluation process of all formulas mentioned above, elimination of unimportant or low import estimators, by use of coefficient of relatively importance C_{RI}, defined by equation (12), by assumption $C_{RI}>0.01$ was done. This process resulted in the elimination of 9 (* - Table 1) and 12 (^ - Table 1) measuring points for main F_C and normal F_N cutting force respectively, for which the residuals ΔF were lying outside the range of about $-3\cdot S_D>\Delta F>3\cdot S_D$. It has to be mentioned that by low value of the C_{RI}, the importance of that estimator was not large.

$$C_{RI}=\left(S_K-S_{KCK0}\right)\cdot S_K^{-1}\cdot 100 \qquad (\%) \qquad (12)$$

In equation (12) the new terms are:

S_{KCK0} - Summation of square of residuals, by $c_K=0$.

c_K - Estimator with number k index in statistical formula evaluated.

The summation of residuals square S_K, the standard deviation S_D, the square of correlation coefficient of the predicted, and observed values R^2 were used for

characterization of the approximation quality. Calculations were performed at Poznań Networking & Supercomputing Center PCSS on a SGI Origin 3800 computer, using a special optimization program, based on a least squares method combined with gradient and Monte Carlo methods, mentioned in the work Porankiewicz (1988), (modified many times in order to improve calculation efficiency). For checking every statistical formula mentioned earlier, as well as for evaluation of the final equations (6) through (8) and (9) through (11), the necessary iteration number was as large as $9.3 \cdot 10^9$ (2200 h).

The authors also decided to check the fitting of Equations (3) through (5) using the experimental matrix applied in the present work. However, the lack of information about the exact number of measuring points used in the work of Axelsson et al. (1993) precluded precise comparison.

For presentation of the estimators evaluated for Equations (6) through (8) and (9) through (11), five decimal digits were assumed, which caused negligible deterioration in the quality of approximation. Reduction in the number of decimal digits to 4 worsened the quality of approximation of equation (6) through (8) and (9) through (11) as much as 0.01% and 8%, respectively. Reduction the number of decimal digits to 2 worsened the quality of approximation of equation (6) through (8) and (9) through (11) as much as 6389% and 649124% respectively.

A comparison of results obtained in the present work with similar data from the literature was carried out. To conduct the comparison, the Wood_Cutting program (Porankiewicz 2011) was used for calculation of the main F_C and radial F_N cutting forces.

RESULTS AND DISCUSSION

For equation (6) through (8), describing the relation $F_C=f(\varphi_V, \rho, \gamma_F, a_p, v_C, D, m_C, T)$, the following estimators resulted from the evaluation: a_1=224914.765, $a_2=6.411 \cdot 10^{-5}$, a_3=-0.04709, a_4=18.90097, a_5=2.57193, a_6=10.57092, a_7=0.0955, a_8=0.15203, a_9=1.17260, a_{10}=-2.15734, a_{11}=-0.05021; a_{12}=-0.07183, a_{13}=2.43628, a_{14}=0.99865, $a_{15}=6.883 \cdot 10^{-5}$, a_{16}=-27269.686, a_{17}=0.02962, a_{18}=0.4157, a_{19}=-0.17439, a_{20}=0.23563, a_{21}=0.19386, a_{22}=1.21835, a_{23}=-0.57335, a_{24}=-0.24134, a_{25}=-878.18, a_{26}=0.01668, a_{27}=-27.65757.

The quality of the fit of the equation (6) through (8) is shown by Fig. 6, and was characterized by the quantifiers: S_K=57722.3, R=0.95, R^2=0.91, S_D=11.87 N. The coefficients of relative importance took values as follows: C_{RI1}=155.7, C_{RI2}=347.9, C_{RI3}=107.7, C_{RI4}=650.3, C_{RI5}=469.9, C_{RI6}=5533.7, C_{RI7}=718.6, C_{RI8}=826, C_{RI9}=940.4 C_{RI10}=219.2, C_{RI11}=108.9, C_{RI12}=113.1, C_{RI13}=226.2, C_{RI14}=225.6, C_{RI15}=338.2, C_{RI16}=7374.3, C_{RI17}=111.2, C_{RI18}=884.6, C_{RI19}=269.7, C_{RI20}=749.2, C_{RI21}=884.6, C_{RI22}=3309.9, $C_{RI23}=1.732 \cdot 10^{12}$, C_{RI24}=1194.8, $C_{RI25}=2.188 \cdot 10^5$, C_{RI26}=169.7, C_{RI27}=645.

The following estimators were evaluated for formulas (9) through (11), describing the relation $F_N=f(\varphi_V, \rho, \gamma_F, a_p, v_C, D, m_C, T)$: $b_1=3.355 \cdot 10^{-3}$, b_2=539082.961, b_3=-0.15741, b_4=-0.33883, b_5=-0.01213, b_6=758.29345, b_7=0.76858, b_8=3.5537, $b_9=5.365 \cdot 10^{-4}$, $b_{10}=1.3538 \cdot 10^{-3}$, $b_{11}=-3.0279 \cdot 10^{-3}$, $b_{12}=-1.3297 \cdot 10^{-4}$, b_{13}=-0.012783, b_{14}=-30.16633, b_{15}=-0.219799, b_{16}=10.134443, $b_{17}=3.4903 \cdot 10^{-4}$, b_{18}=-0.38895, b_{19}=-0.27925, b_{20}=1.90555, b_{21}=-0.10358, b_{22}=-0.732, b_{23}=-0.32493, b_{24}=-0.2652, b_{25}=-137.7076, $b_{26}=-3.6111 \cdot 10^{-3}$,

and b_{27}=1.66647. The quality of the fit of the equation (9) through (11) were characterized by the quantifiers: S_K=45551.2, R=0.93, R^2=0.86, S_D=10.65 N, and also are illustrated in Fig. 6. The coefficients of relative importance took the following values: C_{RI1}=5.809·10^6, C_{RI2}=185.1, C_{RI3}=18.7, C_{RI4}=28, C_{RI5}=14.4, C_{RI6}=547.4, C_{RI7}=711.3, C_{RI8}=1469.7, C_{RI9}=7.1, C_{RI10}=18.7, C_{RI11}=293.3, C_{RI12}=1.3, C_{RI13}=4.028·10^4, C_{RI14}=7.688·10^9, C_{RI15}=4397.8, C_{RI16}=4.368·10^{10}, C_{RI17}=765.6, C_{RI18}=256.7, C_{RI19}=66.8, C_{RI20}=662.8, C_{RI21}=135.8, C_{RI22}=6.312·10^6, C_{RI23}=1471, C_{RI24}=305.1, C_{RI25}=3.059·10^7, C_{RI26}=0.01, C_{RI27}=2.5.

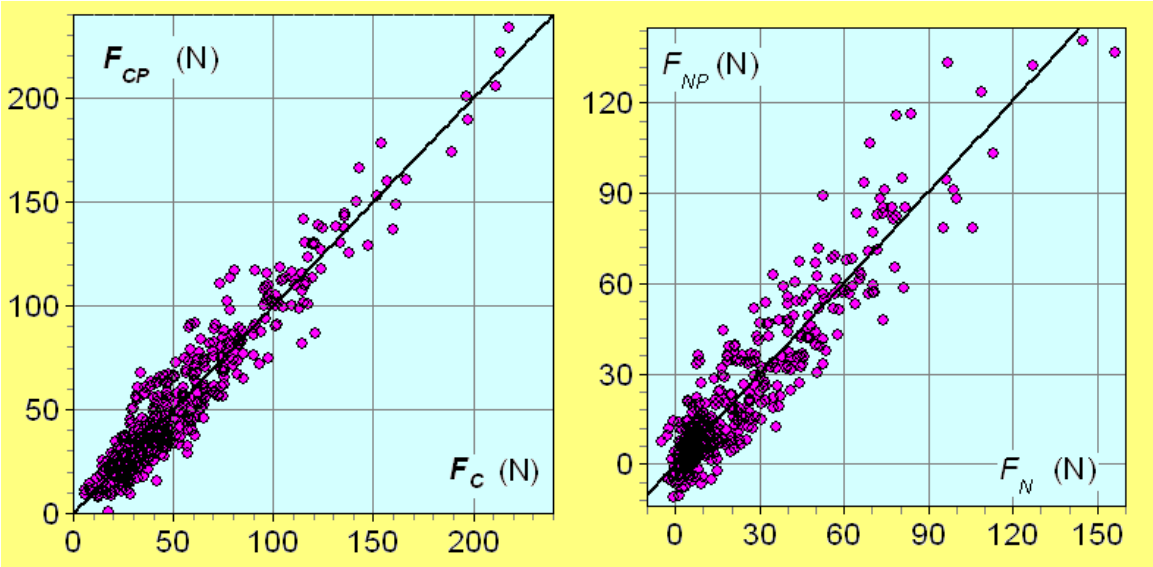

Fig. 6. Plot of main cutting force observed F_C, against main cutting force predicted F_{CP}, according to equations (6) through (8), and the plot of normal cutting force observed F_N, against predicted normal force F_{NP}, according to equations (9) through (11)

Figure. 6 shows that in the analyzed experiment the standard deviation S_D was rather high, which suggested the presence of an uncontrolled variation, and, maybe also an effect of unrecognized interactions. In the authors' opinion more work in future experiments will be needed to reduce the value of S_D. The quality of approximation obtained in the present work for the main force F_C, namely R=0.95, R^2=0.91, was slightly better than for the normal force F_N, namely R=0.93, R^2=0.86, and, much better than the quality of approximation of the equation (3) through (5) for the main force F_C, namely R=0.2, reported in the work Axelsson et al. (1993). Such a good approximation confirms the exceptional precision of optimization method and program applied in this study.

From Fig. 7 can be seen a fast growth of the main force F_C with an increase of the grain angle φ_V, from φ_V =0° up φ_V =1.475312 rad (84.53°), being maximum for cutting against grains case. This observation contradicted information from the literature, reporting the maximum at $\varphi_V = \pi/2$ rad (90°). The maximum in the dependence $F_C=f(\varphi_V)$ can be seen for whole range of variation of the cutting edge dullness ρ. Further rise of the φ_V angle resulted in rapid drop of the F_C. From Fig. 7 can also be seen fast growth of the normal cutting force F_N with an increase of the grain angle φ_V, up to maximum at φ_V=0.801795 rad (45.94°) but only for large cutting edge dullness of ρ=20 μm. This

finding contradicts information reported in the literature (Amalitskij and Lûbčenko 1977; Orlicz 1982). The maximum for the normal cutting force F_N, observed for cutting edge dullness of ρ=20 μm, disappeared for the sharp tool by ρ=5 μm. Further increase of the φ_V angle up to φ_V=1.5708 rad (90°) caused rapid decrease of the F_N, up to minimum. An increase of the φ_V angle, by φ_V>1.5708 rad (90°) (cutting along grains case) resulted in rather small change of the F_N value. This observation was in agreement with the paper of Porankiewicz et al. (2007) and contradicts other information from the literature (Amalitskij and Lûbčenko 1977; Orlicz 1982).

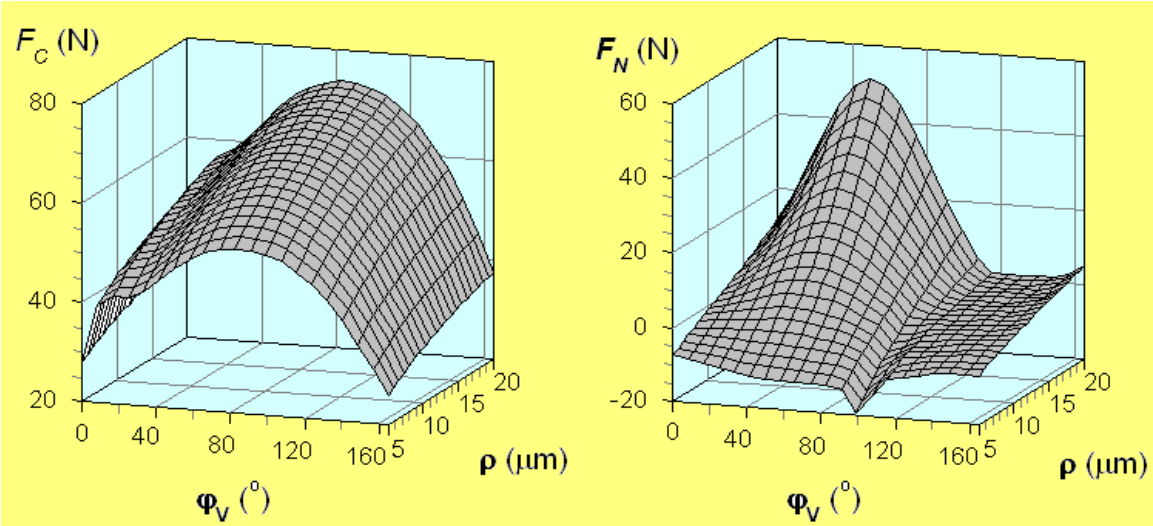

Fig. 7. Plot of dependence of the main F_C and normal F_N cutting forces upon the angle φ_V and the round up of the cutting edge ρ, according to equations: a - (6) through (8); and b – (9) through (11); for: γ_F=0.52 rad (29.79°); a_p=0.5 mm; v_c=39.74 m·s^{-1}; m_c=10 %; D=372 kg·m^{-3}; T=293°K (20°C)

The ratio between maximum and minimum values of the main force F_C for the grain angle φ_V lying in the range of 1.464 rad and 0 rad (84.53° and 0°), was as high as 1.84 in the present study, while as large as 2.62 according to the literature (Orlicz 1982), for the following cutting conditions: ρ=6 μm, γ_F=0.349066 rad (20°), a_P=0.2 mm, v_C=28 m·s^{-1}, m_C=8 %, T=293°K (20°C), and D=490 kg·m^{-3}.

The ratio between maximum and minimum values of the normal force F_C for the grain angle φ_V lying in the range of 0.792 rad and 0 rad (45.94° and 0°), was as high as 2.51 in the present study, while as large as 2.62 according to the literature (Orlicz 1982), for the following cutting conditions: ρ=20 μm, γ_F=0.349066 rad (20°), a_P=0.2 mm, v_C=28 m·s^{-1}, m_C=8 %, T=293°K (20°C), and D=490 kg·m^{-3}.

The ratio between maximum and minimum value of the main force F_C for the largest and the lowest cutting edge round-up ρ, which were as high as 6 μm and 20 μm, respectively, were as high as 1.35 in this paper, while 1.12 according to the literature (Amalitskij and Lûbčenko 1977, Orlicz 1982), for following cutting conditions: φ_V=0.7854 rad (45°), γ_F=0.349066 rad (20°), a_P=0.2 mm, v_C=28 m·s^{-1}, m_C=8 %, T=293°K (20°C), D=490 kg·m^{-3}. The ratio between maximum and minimum value of the radial force F_N for the largest and the lowest cutting edge round-up ρ, were as high as 15.37 in

this paper, while 2.03 according to the literature (Amalitskij and Lûbčenko 1977, Orlicz 1982), for same cutting conditions.

Graphical illustration of the relations (6) though (11) between the main F_C and the normal F_N cutting forces and the rake angle γ_F and the thickness of the cutting layer a_P, are shown in Fig. 8. It can be seen from Fig. 8 that a decrease of the rake angle γ_F increased the main F_C and the normal F_N cutting forces, in a parabolic, increasing manner.

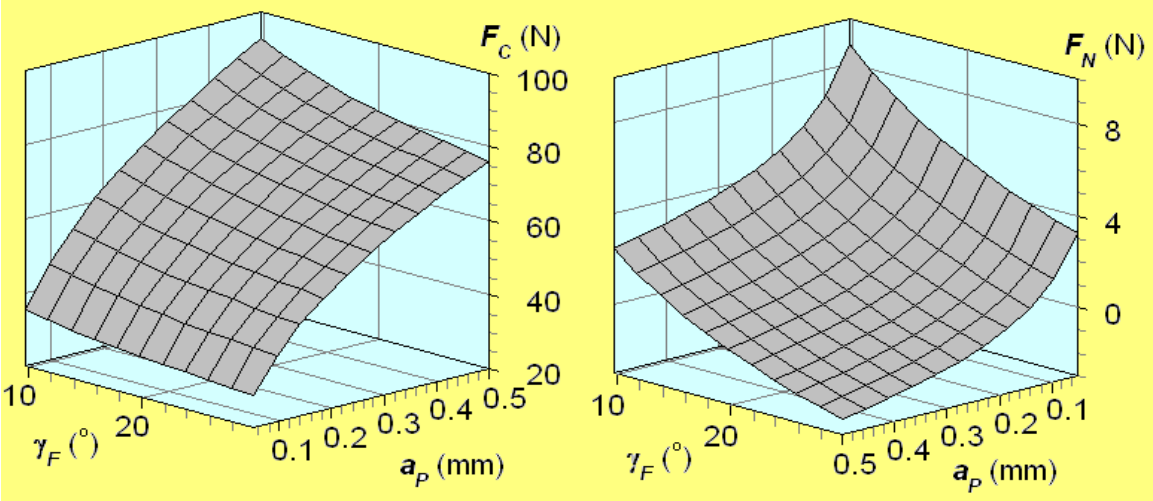

Fig. 8. Plot of dependence of the main F_C and normal F_N cutting forces upon the rake angle γ_F and the thickness of the cutting layer a_P, according to equations: a - (6) though (8); and b - (9) though (11); for φ_V=1.475412 rad (84.53º); ρ=5 μm; v_C=39.74 m·s^{-1}; m_C=10 %; T=293ºK (20ºC); D=500 kg·m^3

An increase of the thickness of the cutting layer a_P resulted in an increase of the main cutting force F_C in parabolic, decreasing manner. An increase of the thickness of the cutting layer a_P resulted in an increase of absolute value of the radial cutting force F_N in parabolic, decreasing manner. It has also to be mentioned that the radial cutting force F_N for some values of the rake angle γ_F and thickness of the cutting layer a_P become positive. The issue of the impact the rake angle γ_F and the thickness of the cutting layer a_P on the the radial cutting force F_N contradicted information from literature (Orlicz 1982).

The ratio between maximum and minimum value of the main force F_C for the largest and the lowest rake angle γ_F, of 0.17 rad (9.74º) and of 0.52 rad (29.79º) respectively, was as large as 1.23 in the present study, while according to the literature (Orlicz 1982) was as large as 1.96, for the following cutting conditions: ρ=6 μm, a_P=0.2 mm, v_C=28 m·s^{-1}, m_C=8 %, T=293ºK (20 ºC), D=490 kg·m^{-3}.

For the same cutting parameters, the ratio between the largest and the lowest value of the radial force F_N was as high as 2.67 in the present study, while as large as 1.96 according to the literature (Orlicz 1982). It has to be mentioned that the radial force F_N evaluated from equation (9) though (11) took negative values in analyzed range of variation of the rake angle γ_F, while the radial force F_N calculated on basis of the equation (1) through (2), according to the literature (Orlicz 1982) was positive.

The ratio between maximum and minimum value of the main force F_C for the largest and the lowest thickness of cutting layer a_P, as high as 0.05 mm and 0.5 mm respectively, was as high as 2.12 in the present study, while as large as 2.82 according to the literature (Orlicz 1982), for following cutting parameters: ρ=6 μm, γ_F=0.349066 rad (20°), φ_I=0.7854 rad (45°), v_C=28 m·s^{-1}, m_C=8 %, T=293°K (20°C), D=490 kg·m^{-3}.

For the same cutting parameters, the ratio between the largest and the lowest value of the radial force F_N, was as high as 4.58 in the present study, while as large as 2.82 according to the literature (Orlicz 1982). It has to be mentioned that the radial force F_N evaluated from equation (9) through (11) took negative values throughout the analyzed range variation of the thickness of cutting layer a_P, while the radial force F_N calculated from equation (1) through (2) was positive according to the literature (Orlicz 1982).

The impact of the wood density D and the cutting velocity v_C the on the main force F_C and the normal force F_N, according to equations (6) through (11), is illustrated in Fig. 9, which shows a very strong influence, with a parabolic increasing manner. The wood density D impact on the radial F_N cutting force was also very strong, in a parabolic, decreasing manner. The cutting velocity v_C impact on the F_C and F_N cutting forces was smaller (especially on the F_N) in a parabolic, decreasing manner.

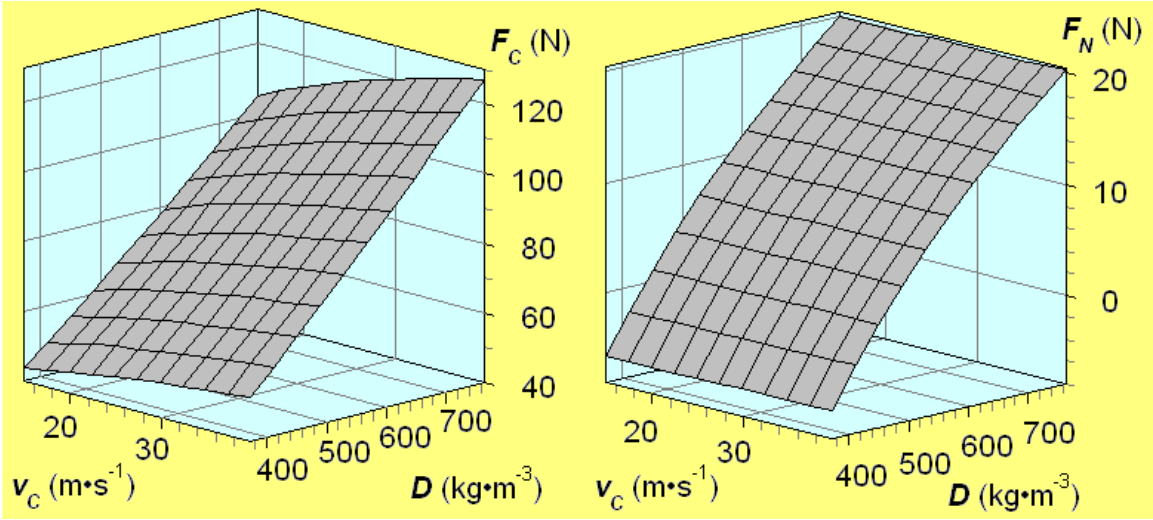

Fig. 9. Plot of the dependence of the main F_C and normal F_N cutting forces upon the wood density D and the cutting velocity v_C, according to equation: a - (6) though (8); and b – (9) though (11); for φ_I=1.475312 rad (84.53°); ρ=5 μm; γ_F=0.349066 rad (20°); a_p=0.5 mm; m_C=8 %; T=293°K (20°C)

As the wood density D increased throughout the analyzed range of variation, the main cutting force F_C increased by as much as 2.49 times, for the following cutting conditions: a_P=0.2 mm, ρ=6 μm, γ_F=0.349066 rad (20°), φ_I=0.7854 rad (45°), v_C=28 m·s^{-1}, m_C=8 %, T=293°K (20°C).

The radial cutting force F_N, for the same cutting conditions, decreased by as much as 1.27 times, in the analyzed range of variation of the wood density D. In the literature the wood density was not taken into account for F_C and F_N cutting forces evaluation (Orlicz 1982).

With an increase of the cutting velocity v_C throughout analyzed variation range from 14.91 m·s^{-1} to 39.74 m·s^{-1}, the main cutting force F_C increased, according to equations (6) though (8) in parabolic, decreasing manner.

An increase of the cutting velocity v_C throughout analyzed range of variation was accompanied by a slight increase in the radial cutting force F_N according to equations (9) through (11) in parabolic, decreasing manner. For low wood density D, the F_N take negative values. The issue of the influence of the cutting velocity v_C on the main F_C and the radial F_N cutting forces contradicted information reported in the literature (Orlicz 1982), giving an opposite influence until v_C=50 m·s^{-1}. The non-linear issue of the impact of the cutting velocity v_C on the main force F_C also was also inconsistent with work Axelsson et al. (1993). Results of the present experiment are unable to explain these contradictions.

The ratio between maximum and minimum value of the main cutting force F_C for the largest and the lowest cutting velocity v_C, as high as 14.91 m·s^{-1} and 39.74 m·s^{-1}, respectively, was as large as 1.54 in the present study, while as much as 0.93 according to the literature (Orlicz 1982), for following cutting conditions: ρ=6 μm, γ_F=0.349066 rad (20°), φ_V=0.7854 rad (45°), a_P=0.2 mm, m_C=8 %, T=293°K (20 °C), D=490 kg·m^{-3}.

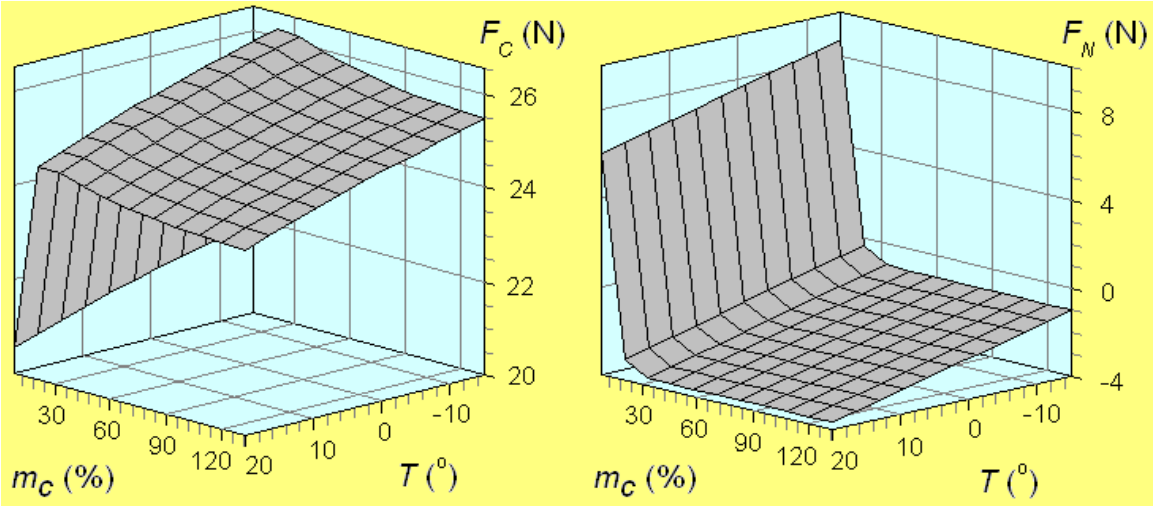

Fig. 10. Plot of dependence of the main F_C and normal F_N cutting forces upon the moisture content m_C, and the wood temperature during cutting T, according to equations: a - (6) though (8); and b – (9) though (11); for φ_V=0 rad (0°); ρ=5 μm; γ_F=0.349066 rad (20°); a_p=0.1 mm; v_C=39.74 m·s^{-1}; D=500 kg·m^{-3}

Figure 10 shows the non-linear dependence of the main F_C and the normal F_N cutting forces upon the moisture content m_C and the wood temperature T. With an increase of the moisture content m_C from 8 % to about 30 % the main force F_C, grew very fast. Further enlargement of the m_C, to 133 %, caused a slightly decrease of the F_C, which was in agreement with the literature (Amalitskij and Lûbčenko 1977; Orlicz 1982) for types of machining other than sawing. The non-linear impact of m_C on the main force F_C issue contradicts the work of Axelsson et al. (1993). For the sawing case, an opposite impact of the moisture content m_C on the cutting forces was reported in the literature (Amalitskij and Lûbčenko 1977; Orlicz 1982). It is well known that there is an

exceptional, increasing effect of the moisture content m_C on the shock strength of wood; indeed, this effect might be invoked to explain this phenomenon at large cutting velocity v_C. However, in the case of sawing (closed cut), an increasing action of the two side edges has to be considered. On the other hand, someone may point out that most of wood's strength properties decrease with increasing moisture content m_C. With the current state of the knowledge it is not possible to estimate which role is dominant in the cutting forces evaluation: wood shock strength or other (static) strengths.

The radial cutting force F_N dependence upon the moisture content m_C was opposite to the dependence observed for the main cutting force F_C in the range from 8 % to about 30 %. This would suggest that the relaxation of the wood surface from the clearance surface site, becomes larger with increasing moisture content m_C in the analyzed range.

The ratio between maximum and minimum value of the F_C, for the moisture content m_C, as high as 8 % and 70 % respectively, was 1.27 in the preset study, while 1.23 according to the literature (Orlicz 1982), for following cutting conditions: ρ=6 μm, γ_F=0.349066 rad (20°), φ_V=0.7854 rad (45°), a_P=0.2 mm, T=293°K (20°C), and D=490 kg·m^{-3}.

For the same machining parameters, the radial force F_N fell with change of the moisture content m_C from value of 4.9 N to -3.5 N, in the present study, while it fell 1.23 times (being positive in whole range) according to the literature (Orlicz 1982).

The main F_C and the normal F_N cutting forces slightly increased with lowering of the wood temperature T (Fig. 9). The ratio between maximum and minimum value of the F_C and for the F_N for the lowest and the highest wood temperature T, as high as 258°K (-15°C) and 293°K (20°C), was as high as 1.06 and 1.59, respectively in this paper, while 1.15 and 1.14 times respectively according to the literature (Orlicz 1982), for following cutting conditions: ρ=6 μm, γ_F=0.349066 rad (20°), φ_V=0.7854 rad (45°), a_P=0.2 mm, m_c=8 %, D=490 kg·m^{-3}.

It has to be pointed out that for another combination of the cutting parameter values, the comparison between models (6) through (11) and (1) through (2) as well as (3) through (5) will bring other values of the ratio.

Figures 7 through 10 show that the normal cutting force F_N did not follow the main cutting force F_C. In case of influence of the thickness of cutting layer a_P, the moisture content m_C and the cutting speed v_C on the radial cutting force F_N (Fig. 10), even a reverse impact was observed, which suggests that the equation (2) was too simple to adequately describe the dependence of the normal force F_N upon cutting parameters.

The impact of the cutting edge dullness ρ, the moisture content m_C, and the cutting speed v_C on the tangential F_C, also the influence of the cutting edge dullness ρ, the rake angle γ_F, the thickness of cutting layer a_P, the moisture content m_C, the wood temperature T, the cutting speed v_C on the radial cutting force F_N in the present study, was larger than that reported in the literature (Amalitskij and Lûbčenko 1977; Orlicz 1982).

The dependence of the main cutting force F_C upon the grain angle φ_V, the rake angle γ_F, the thickness of the cutting layer a_P and the wood temperature T was smaller than that reported in the literature (Amalitskij and Lûbčenko 1977; Orlicz 1982).

The dependence of the radial F_N cutting force upon the grain angle φ_V was smaller than that reported in the literature (Orlicz 1982).

The two-level variation of the cutting edge round up ρ, the cutting velocity v_C, and the wood temperature T independent variables in the experimental matrix of the present study, seemed to not be the best choice, due to their non-linear influence on the main F_C and radial F_N cutting forces.

Different values of the exponents a_9 through a_{13} and b_9 through b_{13} for longitudinal cutting, and, exponents a_{18} through a_{22} and b_{18} through b_{22} for perpendicular cutting, evaluated for equations (6) through (11) showed that the impact of the cutting angle δ_F[1.570796-γ_F] (rad) {[90°-γ_F] (°)}, the cutting edge dullness ρ, the thickness of the cutting layer a_P, the cutting velocity v_C, the moisture content m_C, and the wood temperature T on the tangential F_C and the radial cutting forces F_N was different for these two base cutting directions (perpendicular and longitudinal cutting). The use of the same correction coefficients: C_δ, C_ρ, C_{AP}, C_{VC}, C_{MC}, C_T for longitudinal cutting and for perpendicular cutting in equations (1) perpendicular (2), seems to be one of the reasons reported in literature (Orlicz 1982) to account for differences between predicted and observed main cutting force F_C, decreasing the methods' precision.

The analysis of the relationship (9) through (11) with step 0.0008 rad (0.05°), revealed the existence of a local large extremes at φ_V=1.7282 rad (99.019°). The extremes extend in the range from -0.06981 rad (-4°) to +0.0524 rad (+4°). Because there are no experimental data for the specified range of the φ_V in the experimental matrix, the extremes must be excluded from considerations.

CONCLUSIONS

The analysis of results of the calculations performed makes it possible to state that:

1. The normal cutting force F_N takes a negative value for a wide range of the cutting parameters.
2. In the dependence of the main cutting force F_C upon the grain angle φ_V, a maximum at φ_V=1.475312 rad (84.53°), extending to whole range of variation of the cutting edge dullness ρ, was found.
3. In the dependence of the normal force F_N upon the grain angle φ_V, a maximum was observed at φ_V=0.8017949 rad (45.939°). This maximum disappeared in the case of a sharp tool (ρ=5 μm).
4. An drop down of the rake angle γ_F increased the main F_C and the normal F_N cutting forces, in a parabolic, increasing manner.
5. An increase of the thickness of the cutting layer a_P increased the main cutting force F_C in a parabolic, decreasing manner.
6. An increase of the thickness of the cutting layer a_P increased the absolute value of the radial cutting force F_N in parabolic, decreasing manner.
7. Increasing the wood density D caused an significant increase of the main cutting force F_C in a parabolic, increasing manner.
8. The radial cutting force F_N increased with the wood density D climb in a parabolic, decreasing manner.

9. An increase of the cutting velocity v_C caused an increase of the main cutting force F_C, according to equation (6)-(8), in a parabolic, decreasing manner.
10. An increase of the cutting velocity v_C slightly increased the radial cutting force F_N, according to equation (9) through (11).
11. An increase of the moisture content m_C, in range from 8% to about 30%, resulted in a rapid increase of the main cutting force F_C. A further increase in moisture content m_C to 133% resulted in a further decrease of F_C in parabolic decreasing manner.
12. An increase of the moisture content m_C, in range from 8% to about 30%, resulted in a rapid lowering of the radial cutting force F_N. A very small increase of the absolute value of the F_N was observed in a parabolic increasing manner with the m_C rising to 133%.
13. The main F_C and absolute value of the normal F_N cutting forces slightly increased with a lowering of the wood temperature T, in a parabolic decreasing manner.
14. The dependence of the normal force F_N upon cutting parameters by *Pinus sylvestris* wood cutting does not generally follow the same trends as the main force F_C.
15. In the present work a larger influence of the rake angle γ_F, the cutting edge dullness ρ, the moisture content m_C, and the cutting velocity v_C on the main cutting force F_C was observed, compared to those reported in the literature (Amalitskij and Lûbčenko 1977; Orlicz 1982).
16. In the present work a larger influence of the rake angle γ_F, the cutting edge dullness ρ, the thickness of the cutting layer a_P and the wood temperature T on the radial F_N cutting force was observed than the corresponding dependencies reported in the literature (Orlicz 1982).
17. The dependence the main F_C cutting force upon the grain angle φ_V, the rake angle γ_F, the thickness of the cutting layer a_P, and the wood temperature T was smaller than those given in the literature (Amalitskij and Lûbčenko 1977; Orlicz 1982).
18. The dependence the radial F_C cutting force upon the grain angle φ_V was smaller than those given in the literature (Amalitskij and Lûbčenko 1977; Orlicz 1982).
19. The following issues in the Conclusions of the present study, point ns.: 1, 2, 3, 4, 9, 10, 12 contradicted information from Orlicz (1982).
20. The following issues of non-linear influence of the cutting parameters on the main cutting force F_C in the Conclusions of the present study, point ns.: 5, 7, 9, 11 and 13 contradicted information reported in Axelsson et al. (1993).

ACKNOWLEDGMENTS

The authors are grateful for the support of the Poznań Networking & Supercomputing Center (PCSS), Poznań, Poland for a calculation grant.

REFERENCES CITED

Afanasev, P. S. (1961). *Derevoobrabatyvaûŝie Stanki (Woodworking Machinery)*, Moskva.

Amalitskij, V.,V., and Lûbčenko, V., I. (1977). *Stanki i Instrumenty Derevoobrabatyvaûŝih Predpriâtij (Machinery and tools of woodworking factories)*, Moskva.

Axelsson, B., Lundberg, S., and Grönlund, A. (1993). "Studies of the main cutting force at and near a cutting edge," *Holz als Roh u. Werkstoff* 52, 43-48.

Beršadskij, A. L. (1967). *Razčet Režimov Rezaniâ Drevesiny (Resolution of modes of wood machining)*, Moskva.

Deševoj, M. A. (1939). *Mehaničeskaâ Tehnologâ Dereva (Mechanical technology of wood)*, LTA.

Goli, G., Wyeth D., Atkins A.G., Jeronimidis G., Fioravanti M., Del Taglia A. (2007). "Chip formation in wood cutting with different grain orientations using high and low cutting speeds," AITeM 2007 Conference, Associazione Italiana di Tecnologia Meccanica, Montecatini, September 10-12.

Kivimaa, E. (1950). "The cutting force in woodworking," Rep. No. 18, The State Institute for Technical Research, Helsinki.

McKenzie, W. M. (1961). "Fundamental analysis of the wood cutting process," Dept. of Wood Technology, School of Natural Resources, University of Michigan, Ann Arbor.

Orlicz, T. (1982). *Obróbka Drewna Narzędziami Tnącymi*. (*Machining of wood with use of cutting tools*), Study book SGGW-AR, Warsaw.

Porankiewicz, B., Bermudez, J. C. E., and Tanaka, C. (2007): "Cutting forces by peripheral cutting of low density wood species," *BioResources* 2(4), 671-681.

Porankiewicz, B. (2011). Wood_Cutting, Program in Delphi Borland for calculation of cutting forces, (Not published).

Article submitted: November 28, 2010; Peer review completed: February 17, 2011; Revised version received: July 28, 2011; Accepted: August 1, 2011; Published: August 4, 2011.

APPENDIX

Table 1. Experimental Matrix

F_C (N) 1	F_N (N) 2	F_S (N) 3	φ_V (rad) 4	γ_F (rad) 5	ρ (μm) 6	a_P (mm) 7	m_C (%) 8	T (°C) 9	D (kg·m^{-3}) 10	v_C (m·s^{-1}) 11
23	-3.7	1.2	2.88	0.35	20	0.15	8	20	372.53	39.741
13.5	-0.9	-0.9	2.88	0.52	20	0.15	8	20	386.2	39.741
102.1	-44.3	-4.4	2.36	0.17	20	0.5	8	20	496.56	39.741
83.7	-28.2	2.7	2.36	0.35	20	0.5	8	20	481.2	39.741
117.9	-34.2	6.7	2.36	0.35	20	0.5	8	20	568.63	39.741
81.3	-5.2	6.6	2.36	0.52	20	0.5	8	20	651.93	39.741
79.1	-6.6	3.8	2.88	0.17	20	0.5	8	20	476.36	39.741
60.3	-1.8	3	2.88	0.35	20	0.5	8	20	476.36	39.741
36.7	5.1	-4.9	2.88	0.52	20	0.5	8	20	460.93	39.741
54.4	-3.7	2	2.88	0.17	20	0.5	8	20	392.96	39.741
15.8	-2.5	-0.9	2.88	0.35	20	0.5	8	20	392.96	39.741
29.3	4.1	-2.7	2.88	0.52	20	0.5	8	20	392.96	39.741
129.591	8.056	-1.777	1.57	0.35	5	0.5	40.96	20	715.51	14.916
40.561	-14.765	-1.933	1.57	0.35	5	0.05	48.98	20	722.28	14.916
160.693	-25.839	-6.268	1.57	0.35	20	0.5	64.65	20	710.01	14.916
70.84	-67.838	-3.682	1.57	0.35	20	0.05	106.33	20	683.1	14.916
130.404	-4.431	-4.167	1.57	0.17	5	0.5	100.09	20	640.9	14.916
33.449	-12.862	-1.298	1.57	0.17	5	0.05	83.91	20	691.02	14.916
189.348	-46.98	0.526	1.57	0.17	20	0.5	59.80	20	735.5	14.916
80.01	-85.349	-0.64	1.57	0.17	20	0.05	45.44	20	726.78	14.916
137.999	11.013	-0.402	1.57	0.35	5	0.5	118.56	20	655.26	39.741
37.068	-10.217	-1.568	1.57	0.35	5	0.05	108.16	20	670.28	39.741
200.265	-20.248	-14.438	1.57	0.35	20	0.5	62.60	20	696.05	39.741
75.438	-61.57	-3.983	1.57	0.35	20	0.05	48.66	20	692.16	39.741
177.826	-0.428	-1.757	1.57	0.17	5	0.5	45.73	20	671.96	39.741
37.552	-11.268	-1.943	1.57	0.17	5	0.05	55.27	20	691.82	39.741
233.838	-47.674	5.413	1.57	0.17	20	0.5	83.54	20	682.3	39.741
81.445	-70.718	4.507	1.57	0.17	20	0.05	121.40	20	640.43	39.741
126.492	-2.346	-3.888	1.57	0.35	5	0.5	103.83	-15	694.91	14.916
36.861	-14.183	-1.677	1.57	0.35	5	0.05	48.60	-15	681.02	14.916
148.838	-33.747	-4.703	1.57	0.35	20	0.5	41.92	-15	658.74	14.916
65.808	-63.934	-3.712	1.57	0.35	20	0.05	32.58	-15	647.14	14.916
33.263	-13.325	-1.559	1.57	0.17	5	0.05	45.02	-15	688.6	14.916
173.62	-54.042	-0.922	1.57	0.17	20	0.5	65.86	-15	677.73	14.916
81.564	-82.258	0.641	1.57	0.17	20	0.05	114.01	-15	644.12	14.916
152.509	4.504	-3.439	1.57	0.35	5	0.5	37.06	-15	702.89	39.741
39.857	-12.925	-2.369	1.57	0.35	5	0.05	46.97	-15	718.66	39.741
205.698	-12.468	-8.805	1.57	0.35	20	0.5	80.13	-15	702.49	39.741
68.175	-56.639	-3.909	1.57	0.35	20	0.05	118.81	-15	664.58	39.741
39.876	-13.343	-1.39	1.57	0.17	5	0.05	73.46	-15	627.21	39.741
221.891	-47.702	-0.45	1.57	0.17	20	0.5	56.90	-15	640.23	39.741
88.266	-83.151	1.124	1.57	0.17	20	0.05	34.57	-15	657.4	39.741
101.829	-31.949	-1.626	1.57	0.35	5	0.5	8	-15	567.29	14.916
43.727	-34.75	-1.784	1.57	0.35	5	0.05	8	-15	566.55	14.916
99.88	-43.049	-5.636	1.57	0.35	20	0.5	8	-15	576.48	14.916
50.012	-59.582	-3.249	1.57	0.35	20	0.05	8	-15	572.06	14.916

F_C (N) 1	F_N (N) 2	F_S (N) 3	φ_V (rad) 4	γ_F (rad) 5	ρ (μm) 6	a_P (mm) 7	m_c (%) 8	T (°C) 9	D (kg·m^{-3}) 10	v_C (m·s^{-1}) 11
112.652	-17.168	-3.148	1.57	0.17	5	0.5	8	-15	658.21	14.916
35.153	-18.649	-2.005	1.57	0.17	5	0.05	8	-15	698	14.916
136.268	-42.923	-1.306	1.57	0.17	20	0.5	8	-15	708.93	14.916
64.664	-85.244	-2.725	1.57	0.17	20	0.05	8	-15	595.61	14.916
116.888	-24.582	-2.794	1.57	0.35	5	0.5	8	-15	556.76	39.741
46.011	-34.298	-2.495	1.57	0.35	5	0.05	8	-15	556.96	39.741
117.503	-49.211	-6.215	1.57	0.35	20	0.5	8	-15	545.82	39.741
58.443	-62.678	-2.835	1.57	0.35	20	0.05	8	-15	541.19	39.741
111.886	-22.852	-3.85	1.57	0.17	5	0.5	8	-15	560.65	39.741
36.842	-20.681	-2.164	1.57	0.17	5	0.05	8	-15	567.76	39.741
129.061	-66.835	-2.507	1.57	0.17	20	0.5	8	-15	568.03	39.741
67.81	-81.328	-2.834	1.57	0.17	20	0.05	8	-15	570.71	39.741
113.223	-21.4	-1.644	1.57	0.35	5	0.5	8	20	605	14.916
45.227	-35.825	-1.616	1.57	0.35	5	0.05	8	20	585.54	14.916
113.54	-37.182	-3.752	1.57	0.35	20	0.5	8	20	591.78	14.916
50.544	-61.19	-2.802	1.57	0.35	20	0.05	8	20	590.04	14.916
89.461	-20.726	-4.134	1.57	0.17	5	0.5	8	20	570.31	14.916
32.644	-18.586	-1.492	1.57	0.17	5	0.05	8	20	587.89	14.916
123.453	-55.876	-2.584	1.57	0.17	20	0.5	8	20	580.58	14.916
62.4	-85 12	-2.064	1.57	0.17	20	0.05	8	20	600.44	14.916
141.263	-12.932	-3.105	1.57	0.35	5	0.5	8	20	708.87	39.741
55.39	-36.28	-2.746	1.57	0.35	5	0.05	8	20	658.81	39.741
137.577	-34.917	-4.975	1.57	0.35	20	0.5	8	20	618.76	39.741
66.058	-68.31	-2.271	1.57	0.35	20	0.05	8	20	606.88	39.741
115.523	-19.78	-4.023	1.57	0.17	5	0.5	8	20	553.47	39.741
36.101	-18.301	-1.964	1.57	0.17	5	0.05	8	20	568.1	39.741
149.93	-54.288	-2.87	1.57	0.17	20	0.5	8	20	577.02	39.741
88.863	2.887	0.448	0	0.35	5	0.5	90.98	20	657.27	39.741
18.813	-5.538	-1.4	0	0.35	5	0.05	101.80	20	644.05	39.741
85.663	-18.04	-2.430	0	0.35	20	0.5	110.10	20	637.21	39.741
22.924	-26.732	-1.944	0	0.35	20	0.05	109.40	20	650.83	39.741
91.102	-13.86	-0.248	0	0.17	5	0.5	117.40	20	641.3	39.741
20.313	-9.793	-1.405	0	0.17	5	0.05	120.10	20	642.51	39.741
86.585	-33.166	4.633	0	0.17	20	0.5	119.30	20	656.6	39.741
29.253	-37.533	-0.163	0	0.17	20	0.05	121.70	20	664.72	39.741
68.77	-1.734	0.508	0	0.35	5	0.5	110.40	20	637.27	14.916
18.362	-7.287	-0.863	0	0.35	5	0.05	108.50	20	662.03	14.916
67.114	-17.156	-0.613	0	0.35	20	0.5	113.40	20	677.4	14.916
24.759	-41.809	-1.631	0	0.35	20	0.05	122.40	20	668.88	14.916
76.661	-7.224	0.062	0	0.17	5	0.5	100.10	20	648.75	14.916
17.66	-9.145	0.252	0	0.17	5	0.05	111.90	20	645.26	14.916
74.339	-33.685	6.663	0	0.17	20	0.5	127.40	20	629.56	14.916
30.053	-51.001	2.022	0	0.17	20	0.05	129.10	20	656.19	14.916
91.426	3.766	-3.488	0	0.35	5	0.5	127.50	-15	649.75	14.916
18.745	-10.382	-1.62	0	0.35	5	0.05	132.80	-15	627.95	14.916
81.774	-26.218	-4.703	0	0.35	20	0.5	126.50	-15	637.41	14.916
27.881	-39.707	-2.968	0	0.35	20	0.05	107.10	-15	713.76	14.916
117.163	-7.061	-3.906	0	0.17	5	0.5	132.40	-15	625.26	14.916
20.172	-15 55	-1.356	0	0.17	5	0.05	126.30	-15	636.8	14.916
110.073	-46.683	0.186	0	0.17	20	0.5	116.70	-15	666.73	14.916
37.405	-57.424	2.582	0	0.17	20	0.05	108.20	-15	684.44	14.916

F_C (N) 1	F_N (N) 2	F_S (N) 3	φ_V (rad) 4	γ_F (rad) 5	ρ (μm) 6	a_P (mm) 7	m_c (%) 8	T (°C) 9	D (kg·m^{-3}) 10	v_C (m·s^{-1}) 11
110.385	4.846	-1.991	0	0.35	5	0.5	122.20	-15	654.79	39.741
23.35	-12.145	-1.454	0	0.35	5	0.05	124.90	-15	648.21	39.741
107.669	-34.342	-4.858	0	0.35	20	0.5	122.30	-15	634.86	39.741
29.34	-42.13	-2.440	0	0.35	20	0.05	105.20	-15	691.15	39.741
23.951	-16.067	-1.75	0	0.17	5	0.05	123.30	-15	658.61	39.741
138.437	-51.609	1.045	0	0.17	20	0.5	124.00	-15	631.97	39.741
36.753	-51.756	-0.546	0	0.17	20	0.05	111.70	-15	678.74	39.741
71.442	-6.745	-2.384	0	0.35	5	0.5	8	-15	765 2	14.916
29.202	-20.582	-1.565	0	0.35	5	0.05	8	-15	652.97	14.916
64.708	-14.736	-3.808	0	0.35	20	0.5	8	-15	645.73	14.916
37.277	-43.628	-3.151	0	0.35	20	0.05	8	-15	660.22	14.916
125.402	-3.324	-5.49	0	0.17	5	0.5	8	-15	580.71	14.916
26.967	-10.355	-2.359	0	0.17	5	0.05	8	-15	552.13	14.916
130.217	-21.02	-2.901	0	0.17	20	0.5	8	-15	510.53	14.916
35.113	-56.749	-2.074	0	0.17	20	0.05	8	-15	526.9	14.916
90.5	1.708	-4.127	0	0.35	5	0.5	8	-15	543.14	39.741
83.634	-3.114	-5.556	0	0.35	5	0.5	8	-15	573.26	39.741
29.053	-14.159	-1.822	0	0.35	5	0.5	8	-15	533.95	39.741
57.9	-2.624	-3.617	0	0.35	5	0.5	8	20	588.36	14.916
25.431	-16.517	-1.873	0	0.35	5	0.05	8	20	575.08	14.916
60.576	-12.378	-4.302	0	0.35	20	0.5	8	20	571.52	14.916
34.628	-49.102	-2.967	0	0.35	20	0.05	8	20	592.12	14.916
136.962	-3.835	-5.27	0	0.17	5	0.5	8	20	581.25	14.916
27.863	-11.748	-1.352	0	0.17	5	0.05	8	20	647.94	14.916
159.789	-27.138	-2.121	0	0.17	20	0.5	8	20	627.61	14.916
50.999	-68.388	-2.382	0	0.17	20	0.05	8	20	623.65	14.916
89.44	5.633	-3.094	0	0.35	5	0.5	8	20	561.86	39.741
22.06	-5.72	-1.727	0	0.35	5	0.05	8	20	583.73	39.741
87.818	-7.962	-6.163	0	0.35	20	0.5	8	20	575.34	39.741
33.251	-41.88	-3.535	0	0.35	20	0.05	8	20	650.49	39.741
130.23	-4.862	-8.375	0	0.17	5	0.5	8	20	594.67	39.741
28.466	-14.582	-1.833	0	0.17	5	0.05	8	20	572.26	39.741
166.312	-41.098	-0.928	0	0.17	20	0.5	8	20	583.66	39.741
54.838	-89.148	-1.881	0	0.17	20	0.05	8	20	588.09	39.741
20.5	-4.3	-0.1	0	0.17	5	0.05	8	20	472.26	39.741
11.1	-0.4	1.2	0	0.35	5	0.05	8	20	472.26	39.741
8.1	0.3	1.2	0	0.52	5	0.05	8	20	472.33	39.741
0.97	-1.8	0.8	0	0.17	5	0.05	8	20	464.66	39.741
8.8	-0.3	1	0	0.35	5	0.05	8	20	464.66	39.741
7.5	-0.6	0.8	0	0.52	5	0.05	8	20	464.66	39.741
12.4	-5.5	0.6	0.26	0.17	5	0.05	8	20	454.6	39.741
10.3	-2.7	1.1	0.26	0.35	5	0.05	8	20	454.6	39.741
8.3	-1.6	1	0.26	0.52	5	0.05	8	20	454.6	39.741
15.3	-7.1	0.9	0.26	0.17	5	0.05	8	20	495.8	39.741
9.4	-4.1	1.2	0.26	0.35	5	0.05	8	20	385.86	39.741
8.8	-2.5	1.2	0.26	0.52	5	0.05	8	20	644.1	39.741
16.7	-6.9	1	0.79	0.17	5	0.05	8	20	508.86	39.741
15.1	-6.4	1.8	0.79	0.35	5	0.05	8	20	541.6	39.741
14.5	-5.7	1.6	0.79	0.52	5	0.05	8	20	467.43	39.741
15.1	-6.5	0.7	0.79	0.17	5	0.05	8	20	504.3	39.741
14.9	-4.9	1.8	2.36	0.35	5	0.05	8	20	558.43	39.741

F_C (N)	F_N (N)	F_S (N)	φ_V (rad)	γ_F (rad)	ρ (μm)	a_P (mm)	m_c (%)	T (°C)	D (kg·m^{-3})	v_C (m·s^{-1})
1	2	3	4	5	6	7	8	9	10	11
17.2	-6.9	2.4	0.79	0.52	5	0.05	8	20	556.96	39.741
21	-6.7	1.4	1.35	0.17	5	0.05	8	20	464.43	39.741
17.1	-4	2.3	1.35	0.35	5	0.05	8	20	464.43	39.741
19.2	-6.2	2.5	1.35	0.52	5	0.05	8	20	464.43	39.741
26.5	-6.9	1.6	1.35	0.17	5	0.05	8	20	563.8	39.741
21.7	-4.7	2.7	1.35	0.35	5	0.05	8	20	558.9	39.741
35	-20	4.1	1.35	0.52	5	0.05	8	20	558.9	39.741
22.6	-7.5	1.2	1.57	0.17	5	0.05	8	20	438.56	39.741
17.8	-4.7	2.2	1.57	0.35	5	0.05	8	20	438.56	39.741
31.6	-20.8	3.2	1.57	0.52	5	0.05	8	20	438.56	39.741
20.1	-6.8	1	1.57	0.17	5	0.05	8	20	468.83	39.741
17	-5	2.1	1.57	0.35	5	0.05	8	20	468.83	39.741
28.1	-17.2	3.5	1.57	0.52	5	0.05	8	20	476.43	39.741
22.3	-7.7	1.5	1.84	0.17	5	0.05	8	20	472.56	39.741
19.5	-5.6	2.9	1.84	0.35	5	0.05	8	20	472.56	39.741
30.9	-20	2.9	1.84	0.52	5	0.05	8	20	472.56	39.741
25.4	-6.6	1.2	1.84	0.17	5	0.05	8	20	562.56	39.741
21.5	-4.1	2.4	1.84	0.35	5	0.05	8	20	562.56	39.741
26.4	-15.8	2.9	1.84	0.52	5	0.05	8	20	513.7	39.741
36.9	-1.6	2.2	0	0.17	5	0.15	8	20	474.06	39.741
22.7	1.6	2.4	0	0.35	5	0.15	8	20	474.06	39.741
19.7	-1.3	1.7	0	0.52	5	0.15	8	20	474.06	39.741
26.5	-2.2	1.1	0	0.17	5	0.15	8	20	498.46	39.741
14.8	0.6	1.8	0	0.35	5	0.15	8	20	498.53	39.741
9.8	1.3	0.9	0	0.52	5	0.15	8	20	449.76	39.741
41.4	-8.4	2.2	0.26	0.17	5	0.15	8	20	482.46	39.741
31.8	-1.6	3.7	0.26	0.35	5	0.15	8	20	482.46	39.741
26.6	-11.8	2.4	0.26	0.52	5	0.15	8	20	467.33	39.741
31.5	-7.9	2.2	0.26	0.17	5	0.15	8	20	473.2	39.741
23.3	-3	2.7	0.26	0.35	5	0.15	8	20	473.2	39.741
19.6	-9.5	1.9	0.26	0.52	5	0.15	8	20	381.66	39.741
31.4	-8.3	1.7	0.79	0.17	5	0.15	8	20	495.06	39.741
24.6	-2.8	3.4	0.79	0.35	5	0.15	8	20	459.5	39.741
35.1	-14.3	3.5	0.79	0.52	5	0.15	8	20	459.5	39.741
27.7	-7	1.4	0.79	0.17	5	0.15	8	20	499.6	39.741
25	-2.8	2.8	0.79	0.35	5	0.15	8	20	499.6	39.741
31.7	-11.9	2.9	0.79	0.52	5	0.15	8	20	499.6	39.741
41.1	-7.7	2	1.35	0.17	5	0.15	8	20	469.13	39.741
32.7	-0.9	3.6	1.35	0.35	5	0.15	8	20	469.13	39.741
43.2	-11.4	4.3	1.35	0.52	5	0.15	8	20	469.13	39.741
36.6	-8.1	2.1	1.35	0.17	5	0.15	8	20	513.36	39.741
31.6	-1.8	3.4	1.35	0.35	5	0.15	8	20	513.36	39.741
33	-8.2	3.2	1.35	0.52	5	0.15	8	20	540.8	39.741
39.4	-10	2.2	1.57	0.17	5	0.15	8	20	472.23	39.741
33.2	-2.8	3.8	1.57	0.35	5	0.15	8	20	472.23	39.741
41.3	-12.4	4.1	1.57	0.52	5	0.15	8	20	472.23	39.741
36.9	-7.4	1.9	1.57	0.17	5	0.15	8	20	472.4	39.741
33.6	-0.2	3.7	1.57	0.35	5	0.15	8	20	471.3	39.741
36.5	-7.1	4.2	1.57	0.52	5	0.15	8	20	471.3	39.741
42.5	-10.4	1	1.84	0.17	5	0.15	8	20	470.2	39.741
34.8	-3.1	3	1.84	0.35	5	0.15	8	20	470.2	39.741

F_C (N)	F_N (N)	F_S (N)	φ_V (rad)	γ_F (rad)	ρ (μm)	a_P (mm)	m_c (%)	T (°C)	D (kg·m^{-3})	v_C (m·s^{-1})
1	2	3	4	5	6	7	8	9	10	11
38.9	-19.1	3	1.84	0.52	5	0.15	8	20	470.2	39.741
41.7	-6.6	2.2	1.84	0.17	5	0.15	8	20	525.76	39.741
42.2	2.4	4.1	1.84	0.35	5	0.15	8	20	539.03	39.741
42.6	-5.4	1.6	1.84	0.52	5	0.15	8	20	539.03	39.741
81.8	0.7	1.7	0	0.17	5	0.5	8	20	464.4	39.741
51.5	7.8	4	0	0.35	5	0.5	8	20	491.83	39.741
37.1	4.8	2	0	0.52	5	0.5	8	20	399.56	39.741
65.5	-1.4	3.9	0	0.17	5	0.5	8	20	442.36	39.741
44.7	6.2	3.8	0	0.35	5	0.5	8	20	442.36	39.741
29.3	2.8	1.1	0	0.52	5	0.5	8	20	442.36	39.741
104.6	-11.3	0.3	0.26	0.17	5	0.5	8	20	493.76	39.741
77.4	10.8	4.2	0.26	0.35	5	0.5	8	20	493.76	39.741
53.4	6.6	2.5	0.26	0.52	5	0.5	8	20	493.76	39.741
81.2	-4.4	3	0.26	0.17	5	0.5	8	20	445.93	39.741
55.4	4.5	2	0.26	0.35	5	0.5	8	20	445.93	39.741
42.3	-7.3	1.7	0.26	0.52	5	0.5	8	20	391.66	39.741
61.9	-6.8	4	0.79	0.17	5	0.5	8	20	489.2	39.741
55.5	2.9	4.6	0.79	0.35	5	0.5	8	20	489.2	39.741
52.5	-11.6	-0.4	0.79	0.52	5	0.5	8	20	495.06	39.741
83.1	-14.3	-7.2	0.79	0.17	5	0.5	8	20	535.13	39.741
69.3	5.9	4.2	0.79	0.35	5	0.5	8	20	535.13	39.741
68.5	1.4	2.1	0.79	0.52	5	0.5	8	20	573.03	39.741
73.7	-8.3	2.2	1.35	0.17	5	0.5	8	20	473.6	39.741
61	1.7	3.2	1.35	0.35	5	0.5	8	20	473.6	39.741
62	-3.9	1.2	1.35	0.52	5	0.5	8	20	473.6	39.741
75.9	-7	4.3	1.35	0.17	5	0.5	8	20	524.76	39.741
71.2	4.6	3.5	1.35	0.35	5	0.5	8	20	524.76	39.741
74.3	-0.1	0.2	1.35	0.52	5	0.5	8	20	524.76	39.741
85.6	-11.1	0.6	1.57	0.17	5	0.5	8	20	471.3	39.741
78.1	3	4.4	1.57	0.35	5	0.5	8	20	471.3	39.741
74.8	-5.5	1.6	1.57	0.52	5	0.5	8	20	471.3	39.741
86.9	-11.3	1.4	1.57	0.17	5	0.5	8	20	477.46	39.741
57.6	-5.7	-2.2	1.57	0.35	5	0.5	8	20	472.4	39.741
70.2	-5.7	-0.8	1.57	0.52	5	0.5	8	20	476.43	39.741
56	-16	-2.3	1.84	0.52	5	0.5	8	20	526.93	39.741
109.4	-20.1	-8.7	1.84	0.17	5	0.5	8	20	562.56	39.741
69.7	-17.2	-4.9	1.84	0.35	5	0.5	8	20	513.7	39.741
58.6	-22.2	-2	1.84	0.52	5	0.5	8	20	513.7	39.741
15.3	-7.4	0.1	0.79	0.17	5	0.05	8	20	485.7	39.741
14	-6.6	1.6	0.79	0.35	5	0.05	8	20	485.6	39.741
21.5	-13.5	1.2	2.36	0.52	5	0.05	8	20	502.83	39.741
19.9	-8.9	1.2	2.36	0.17	5	0.05	8	20	515.56	39.741
17.6	-6.6	1.7	2.36	0.35	5	0.05	8	20	515.56	39.741
22.5	-14.6	1.4	2.36	0.52	5	0.05	8	20	515.56	39.741
16.9	-1.7	0.4	2.88	0.17	5	0.05	8	20	455.43	39.741
10.6	0.3	1	2.88	0.35	5	0.05	8	20	455.43	39.741
14.3	-2.3	0.8	2.88	0.52	5	0.05	8	20	455.43	39.741
12.2	-2.4	0.6	2.88	0.17	5	0.05	8	20	380.23	39.741
9	-0.2	0.9	2.88	0.35	5	0.05	8	20	380.23	39.741
11.6	-2.5	0.9	2.88	0.52	5	0.05	8	20	391.56	39.741
39.1	-9.9	1.6	2.36	0.17	5	0.15	8	20	526.83	39.741

F_C (N)	F_N (N)	F_S (N)	φ_V (rad)	γ_F (rad)	ρ (μm)	a_P (mm)	m_c (%)	T (°C)	D (kg·m^{-3})	v_C (m·s^{-1})
1	2	3	4	5	6	7	8	9	10	11
33.8	-4.6	4	2.36	0.35	5	0.15	8	20	526.83	39.741
39.8	-9.9	2.9	2.36	0.52	5	0.15	8	20	523.26	39.741
34.8	-9.5	0.2	2.36	0.17	5	0.15	8	20	551.63	39.741
29	-4	2.4	2.36	0.35	5	0.15	8	20	551.63	39.741
35.2	-12.7	0.4	2.36	0.52	5	0.15	8	20	551.63	39.741
26.4	-0.7	0.7	2.88	0.17	5	0.15	8	20	464.76	39.741
24	1	1.4	2.88	0.35	5	0.15	8	20	478.43	39.741
22.7	1.3	0.6	2.88	0.52	5	0.15	8	20	478.43	39.741
22.4	-0.1	1	2.88	0.17	5	0.15	8	20	397.93	39.741
13.8	1.5	1.9	2.88	0.35	5	0.15	8	20	397.93	39.741
10.6	1.1	0.5	2.88	0.52	5	0.15	8	20	397.93	39.741
82.3	-33	-11.7	2.36	0.17	5	0.5	8	20	497.16	39.741
62.6	-19.9	-3.2	2.36	0.35	5	0.5	8	20	497.16	39.741
32.5	-14	-6.1	2.36	0.52	5	0.5	8	20	497.16	39.741
91.1	-36.3	-13.4	2.36	0.17	5	0.5	8	20	500.33	39.741
73.9	-17	-2.8	2.36	0.35	5	0.5	8	20	500.33	39.741
73	-20.6	-6.4	2.36	0.52	5	0.5	8	20	500.33	39.741
63.7	-10.3	-6.2	2.88	0.17	5	0.5	8	20	478.3	39.741
21.4	-1.7	-1.2	2.88	0.35	5	0.5	8	20	459.8	39.741
17	1	-1.5	2.88	0.52	5	0.5	8	20	459.8	39.741
42.4	-2.8	-2.8	2.88	0.17	5	0.5	8	20	400.2	39.741
28.4	3.3	0.1	2.88	0.35	5	0.5	8	20	400.2	39.741
23.6	5.7	-0.6	2.88	0.52	5	0.5	8	20	400.2	39.741
27.3	-54.4	1.8	0	0.17	20	0.05	8	20	521.9	39.741
27.5	-67	2.6	0	0.35	20	0.05	8	20	521.9	39.741
27.8	-55.3	-8.1	0	0.52	20	0.05	8	20	521.9	39.741
17.7	-33.3	0.7	0	0.17	20	0.05	8	20	624.7	39.741
11.5	-32.3	1.4	0	0.35	20	0.05	8	20	624.7	39.741
10.5	-24.2	1.2	0	0.52	20	0.05	8	20	624.7	39.741
36.1	-91.1	0.4	0.26	0.17	20	0.05	8	20	433.33	39.741
37.3	-95	2	0.26	0.35	20	0.05	8	20	433.33	39.741
36.3	-82.9	-1.3	0.26	0.52	20	0.05	8	20	433.33	39.741
38.1	-94.6	-0.9	0.26	0.17	20	0.05	8	20	461.06	39.741
32.3	-77.1	0.4	0.26	0.52	20	0.05	8	20	461.06	39.741
60.8	-136.5	0.3	0.79	0.17	20	0.05	8	20	464.06	39.741
55.4	-132.6	-2	0.79	0.35	20	0.05	8	20	464.06	39.741
50.1	-103	0.9	0.79	0.52	20	0.05	8	20	464.06	39.741
65.7	-140.7	-3.9	0.79	0.17	20	0.05	8	20	535.23	39.741
48.3	-123.5	-3.6	0.79	0.35	20	0.05	8	20	646.8	39.741
56.9	-78.3	-3.7	0.79	0.52	20	0.05	8	20	535.23	39.741
40.4	-58.6	2.4	1.35	0.35	20	0.05	8	20	487.16	39.741
63.4	-133.4	-4.7	1.35	0.17	20	0.05	8	20	522.6	39.741
56.3	-71	2.2	1.35	0.52	20	0.05	8	20	558.9	39.741
47.2	-57	3.6	1.57	0.17	20	0.05	8	20	470.23	39.741
42.5	-58.4	1.5	1.57	0.35	20	0.05	8	20	470.23	39.741
28.4	-56.9	-3.2	1.57	0.17	20	0.05	8	20	490.4	39.741
36.7	-44.1	3.1	1.84	0.35	20	0.05	8	20	510.23	39.741
47.3	-58.7	-1.3	0	0.17	20	0.15	8	20	491.83	39.741
33.9	-53.5	1.6	0	0.35	20	0.15	8	20	491.83	39.741
28.4	-42.3	1.4	0	0.52	20	0.15	8	20	491.83	39.741
33.2	-35.4	2.1	0	0.17	20	0.15	8	20	449.76	39.741

F_C (N)	F_N (N)	F_S (N)	φ_V (rad)	γ_F (rad)	ρ (μm)	a_P (mm)	m_c (%)	T (°C)	D (kg·m^{-3})	v_C (m·s^{-1})
1	2	3	4	5	6	7	8	9	10	11
20.4	-25.5	1.2	0	0.35	20	0.15	8	20	449.76	39.741
21.6	-33.9	1	0	0.52	20	0.15	8	20	451.96	39.741
46.2	-83.2	-1.7	0.26	0.17	20	0.15	8	20	473.2	39.741
44.8	-56.5	2.9	0.26	0.35	20	0.15	8	20	473.2	39.741
31.5	-58.2	7.4	0.26	0.52	20	0.15	8	20	381.66	39.741
50.8	-88.1	-7.4	0.79	0.17	20	0.15	8	20	495.06	39.741
56.4	-91	0.6	0.79	0.52	20	0.15	8	20	459.5	39.741
61.2	-78.6	-15.6	0.79	0.17	20	0.15	8	20	559.66	39.741
52.1	-65.2	-14	0.79	0.35	20	0.15	8	20	559.66	39.741
56.7	-93.5	-5	0.79	0.52	20	0.15	8	20	646.8	39.741
45.8	-69.3	-5.9	1.35	0.35	20	0.15	8	20	487.16	39.741
45.4	-62.2	-6.7	1.35	0.52	20	0.15	8	20	487.16	39.741
84.7	-56.5	2.4	1.35	0.17	20	0.15	8	20	518.76	39.741
73.1	-56.7	4.7	1.35	0.35	20	0.15	8	20	521	39.741
53.3	-71.5	-4.1	1.35	0.52	20	0.15	8	20	540.8	39.741
58.1	-41.4	3.3	1.57	0.17	20	0.15	8	20	470.56	39.741
45.3	-35.2	3.3	1.57	0.35	20	0.15	8	20	470.23	39.741
47.6	-31.9	1.5	1.57	0.52	20	0.15	8	20	470.23	39.741
44.6	-30.2	2.2	1.57	0.17	20	0.15	8	20	427.40	39.741
57.9	-33	4.2	1.57	0.35	20	0.15	8	20	495.86	39.741
45.7	-22.7	0.4	1.57	0.52	20	0.15	8	20	441.1	39.741
45.5	-25.9	2.7	1.84	0.17	20	0.15	8	20	474.63	39.741
44.5	-30.7	2.7	1.84	0.35	20	0.15	8	20	467.86	39.741
48.8	-29.5	1.3	1.84	0.52	20	0.15	8	20	467.86	39.741
56.5	-31.1	3	1.84	0.17	20	0.15	8	20	530.16	39.741
100.6	-15.9	2.4	0	0.17	20	0.5	8	20	522.93	39.741
60.1	-15.8	2	0	0.35	20	0.5	8	20	522.93	39.741
44.7	-7.2	0.6	0	0.52	20	0.5	8	20	456.86	39.741
90.4	-12	0.9	0	0.17	20	0.5	8	20	482.36	39.741
49.5	-7.7	2.4	0	0.35	20	0.5	8	20	482.36	39.741
53.8	-18.5	-8.9	0	0.52	20	0.5	8	20	451.96	39.741
110	-60.5	-2	0.26	0.17	20	0.5	8	20	470.36	39.741
97.7	-62.6	3.9	0.26	0.35	20	0.5	8	20	470.5	39.741
75	-32.2	-2.7	0.26	0.52	20	0.5	8	20	470.36	39.741
73	-35.1	7.9	0.26	0.17	20	0.5	8	20	385.86	39.741
56.4	-23.8	-0.1	0.26	0.52	20	0.5	8	20	385.86	39.741
113	-58.7	3.6	0.79	0.17	20	0.5	8	20	541.6	39.741
99.3	-51.5	3.9	0.79	0.35	20	0.5	8	20	541.6	39.741
89.6	-35.8	0.7	0.79	0.52	20	0.5	8	20	508.86	39.741
115.8	-53.2	2.6	0.79	0.17	20	0.5	8	20	504.3	39.741
93.6	-38.8	2	0.79	0.35	20	0.5	8	20	504.3	39.741
104.8	-36.5	1.9	0.79	0.52	20	0.5	8	20	556.96	39.741
129.2	-41.9	1.6	1.35	0.17	20	0.5	8	20	502.66	39.741
101.9	-21.8	0.2	1.35	0.52	20	0.5	8	20	506.66	39.741
142.6	-45.7	1.8	1.35	0.17	20	0.5	8	20	558.9	39.741
98.3	-32.6	2.8	1.35	0.35	20	0.5	8	20	533.76	39.741
107.1	-19.1	0.9	1.35	0.52	20	0.5	8	20	570.6	39.741
101.3	-53.3	-0.1	1.57	0.17	20	0.5	8	20	486.66	39.741
99.8	-42.4	2.8	1.57	0.35	20	0.5	8	20	486.66	39.741
87.6	-28.6	0.2	1.57	0.52	20	0.5	8	20	484.33	39.741
144	-36	3	1.57	0.17	20	0.5	8	20	558.46	39.741

F_C (N) 1	F_N (N) 2	F_S (N) 3	φ_V (rad) 4	γ_F (rad) 5	ρ (μm) 6	a_P (mm) 7	m_c (%) 8	T (°C) 9	D (kg·m^{-3}) 10	v_C (m·s^{-1}) 11
90.5	-32.4	3.3	1.57	0.35	20	0.5	8	20	490.16	39.741
83.4	-21.1	-3.3	1.57	0.52	20	0.5	8	20	438.66	39.741
111	-46.9	-3.3	1.84	0.17	20	0.5	8	20	502.33	39.741
101.3	-36.1	1.1	1.84	0.35	20	0.5	8	20	502.33	39.741
102.8	-21.5	-3.1	1.84	0.52	20	0.5	8	20	506.33	39.741
115.4	-46.2	-2.4	1.84	0.17	20	0.5	8	20	495	39.741
109.9	-36.4	4.5	1.84	0.35	20	0.5	8	20	482.66	39.741
100.2	-23.4	-0.9	1.84	0.52	20	0.5	8	20	502.33	39.741
40	-39.3	1.7	2.36	0.17	20	0.05	8	20	526.83	39.741
34.7	-36.1	2.3	2.36	0.35	20	0.05	8	20	523.33	39.741
33	-28.8	2.5	2.36	0.52	20	0.05	8	20	523.33	39.741
39.2	-39.1	-0.3	2.36	0.17	20	0.05	8	20	525.96	39.741
36.9	-39	0.9	2.36	0.35	20	0.05	8	20	525.96	39.741
27.7	-22.8	2.9	2.36	0.52	20	0.05	8	20	569.36	39.741
22.7	-14.5	0.9	2.88	0.17	20	0.05	8	20	464.76	39.741
20.1	-14.7	1.3	2.88	0.35	20	0.05	8	20	464.76	39.741
22.6	-15.5	-0.3	2.88	0.52	20	0.05	8	20	478.43	39.741
24.8	-15.5	2.7	2.88	0.17	20	0.05	8	20	431.33	39.741
20	-14.1	0.5	2.88	0.35	20	0.05	8	20	461.66	39.741
18.3	-8.8	-0.2	2.88	0.52	20	0.05	8	20	461.66	39.741
67.5	-38.8	4.7	2.36	0.17	20	0.15	8	20	514.73	39.741
58	-29.3	4.7	2.36	0.35	20	0.15	8	20	503.66	39.741
55.4	-24	3	2.36	0.52	20	0.15	8	20	503.66	39.741
48.7	-10.2	1.8	2.88	0.17	20	0.15	8	20	499.03	39.741
27	-7.1	1	2.88	0.35	20	0.15	8	20	475.4	39.741
36.7	-8	2.4	2.88	0.17	20	0.15	8	20	372.53	39.741
74.308	-88.17	-1.539	1.57	0.17	20	0.05	8	20	593.66	39.741
39.8	-47.7	1.6	1.35	0.52	20	0.05	8	20	457.3	39.741
72.7	-106.7	-9.2	1.35	0.17	20	0.15	8	20	463.6	39.741
42.7	-115.6	-2.2	0.26	0.35	20	0.05	8	20	461.06	39.741
65.6	-116.5	-5	0.79	0.35	20	0.15	8	20	459.5	39.741
67	-58	1.2	2.36	0.52	20	0.15	8	20	497.4	39.741
53.2	-92.6	-4.3	0.26	0.52	20	0.15	8	20	467.33	39.741
60.7	-102.6	-12	1.57	0.52	20	0.05	8	20	447.66	39.741
62.3	-133.6	-5.3	1.35	0.35	20	0.05	8	20	522.6	39.741
57.4	-107	-4.6	1.57	0.52	20	0.05	8	20	490.4	39.741
78.8	-72.8	3.4	2.36	0.17	20	0.15	8	20	497.4	39.741
63.1	-113.2	-9.8	1.84	0.17	20	0.05	8	20	451.6	39.741
144.49	^-3.263	-6.581	0	0.35	5	0.5	8	-15	539.18	39.741
159.598	^-33.972	-2.276	0	0.35	5	0.5	8	-15	553.6	39.741
283.459	^ 3.741	-7.48	1.57	0.17	5	0.5	124.57	-15	615.6	39.741
27.5	^ -8.6	-1.8	2.36	0.52	20	0.5	8	20	522.13	39.741
36.1	^-11.5	1.1	2.36	0.17	20	0.5	8	20	522.5	39.741
206.79	^ 6.706	-4.433	1.57	0.17	5	0.5	32.53	-15	679.54	14.916
150.272	^-9.531	-4.918	0	0.17	5	0.5	127.90	-15	650.16	39.741
28.909	^-15.205	-1.268	0	0.35	5	0.5	8	-15	581.32	39.741
24.903	^-27.019	-2.564	0	0.35	5	0.5	8	-15	573.87	39.741
29.8	^-2.9	-2.2	1.84	0.17	5	0.5	8	20	465.93	39.741
26.2	^-12.7	-3.9	1.84	0.35	5	0.5	8	20	510.9	39.741
64.5	^-31.8	-0.7	0.26	0.35	20	0.5	8	20	644.1	39.741
56.5	-103.4	-7.4	1.84	0.52	20	0.05	8	20	451.6	39.741

F_C (N)	F_N (N)	F_S (N)	φ_V (rad)	γ_F (rad)	ρ (μm)	a_P (mm)	m_c (%)	T (^{o}C)	D (kg·m^{-3})	v_C (m·s^{-1})
1	2	3	4	5	6	7	8	9	10	11
* 64.1	-134.7	-5.5	1.84	0.17	20	0.05	8	20	510.23	39.741
* 61.4	-130.8	-8.4	1.57	0.35	20	0.05	8	20	490.4	39.741
* 67.8	-136.2	-9.9	1.84	0.35	20	0.05	8	20	451.6	39.741
* 42.5	-54.2	0.9	1.35	0.17	20	0.05	8	20	463.6	39.741
* 72.3	-68.2	3.7	2.36	0.35	20	0.15	8	20	497.4	39.741
* 67.3	-123.2	-7.5	0.26	0.17	20	0.15	8	20	482.46	39.741
* 66	-134.6	-2.8	0.26	0.35	20	0.15	8	20	467.33	39.741
* 53.465	-91.272	-2.656	0	0.35	5	0.5	8	-15	564.27	39.741

F_S - Side cutting force